IN-FLIGHT VALIDATION OF ROTORCRAFT EMISSION PREDICTIONS AND LOW-POLLUTANT MISSION

A. Frassoldati, A. Cuoci, T. Faravelli, Chemistry, Material and Chemical Engineering Department "Giulio Natta" (CMIC), Politecnico di Milano, Milano, Italy

A. Ferrante, Centro Combustione Ambiente S.r.l., Gioia del Colle, Bari, Italy

M. Stachurska, PZL-Świdnik, Świdnik, Poland

M. Redaelli*, L. Riviello, AgustaWestland, Cascina Costa di Samarate, Varese, Italy

* Corresponding author: matteo.redaelli@agustawestland.com, +39 0331 225125

Abstract

This paper deals with the development of a predictive tool to estimate the Rolls-Royce Allison 250-C20B engine emissions, when installed on the PZL SW-4 helicopter. To confirm the prediction capability achieved, an ad-hoc methodology has also been developed for the in-flight measurement of emissions. The results have been critically analysed, with the aim of producing guidelines for low-pollutant light single-engined helicopter missions.

1. INTRODUCTION

Worldwide the aviation industry consumes about 1.5 billion barrels of traditional jet fuel annually. Although today air transport only produces 2% of man-made CO_2 emissions, this is expected to increase to 3% by 2050 with the continuous and steady traffic growth.

The research and development actions to reduce environmental impact and to increase energy efficient propulsion requires a multidisciplinary approach with key industrial partners from aeronautics (engine manufacturers, aircraft manufacturers), fuel industry and research organization covering a large spectrum of expertise in the fields of aeronautics, combustion as well as the capability to carry out comparison tests in realistic conditions. In order to verify the reliability of different approaches to reach those goals a methodology should be developed able to proof the real reduction of environmental impact in realistic condition, and it requires to perform in flight test measurements campaigns. However, to make the results of numerical simulations and test campaign meaningful, standardization of methods and technologies has to be established.

In Clean Sky, a EU-funded research programme, a dedicated subproject, Green Rotorcraft (GRC) 5, has been devoted to the development of innovative green flight paths and a specific task (GRC5 technology product 10) to develop a predictive tool for helicopter engine emission estimation (project EMICOPTER) and to perform in-flight flue gas measurements (project MAEM-RO).

In this paper the software tool developed to estimate the emissions of the Rolls-Royce Allison 250-C20B engine, installed on the PZL SW-4 helicopter, is described. The methodology developed to measure helicopter engine flue gas emissions during ground / in-flight tests is also discussed together with some comparison results from the test campaign.

The success of the test campaign performed allowed to validate the predictive tool and also demonstrated the validity of the methodology developed to perform in-flight measurements.

2. DEVELOPMENT OF A PREDICTIVE TOOL FOR HELICOPTER ENGINE EMISSION ESTIMATION

Direct coupling of detailed kinetics and complex CFD is a very challenging task, especially when considering the typical dimensions of the computational grids used for complex geometries. Anyway, detailed chemistry is absolutely necessary to investigate pollutant formation which are present in few amounts (ppms or ppbs). Pollutant species (but soot) only marginally affect the main combustion, consequently it is feasible to evaluate the structure of the flame with reduced kinetic schemes first and then post-process the CFD results with detailed kinetics. This technique (Reactor Network Analysis-RNA) is known and widely applied. However, in current 'RNA' codes, the fluid dynamics of the system is simplified and reduced to a limited number of chemical reactors in order to use detailed kinetic mechanisms. A newly-conceived numerical tool, called Kinetic Post-Processor (KPPSMOKE) has been developed, improved, parallelized and applied to predict the formation of different pollutants. The KPPSMOKE [1] is based on the general concept of reactor network analysis but extends it far beyond the limits of traditional RNA applications, which are usually restricted to only a few ideal reactors. In fact, in these applications the number of reactors is limited to reduce the number of equations to values less than ~10^5, while the KPPSMOKE code can be applied up to ~10^8 non-linear equations. KPPSMOKE does not depend on any particular CFD code for the fluid dynamic simulations. The main novelty and advantage of this approach lies in its predictive character. No tuning parameters are introduced and this makes the approach more reliable, especially for predictions in conditions where no experimental

information is available. This approach can also drive the design of new combustors, and to address toward new optimized configurations.

2.1. Kinetic mechanism for jet-fuels

The detailed kinetic mechanism for the pyrolysis and combustion of hydrocarbon fuels, developed at Politecnico di Milano (http://creckmodeling.chem.polimi.it/) is here discussed for jet fuels and further validated using recent measurements. This detailed oxidation mechanism of hydrocarbons up to C16, consists of over 10000 reactions and 400 species, was developed based on hierarchical modularity and lumping procedures. The kinetic modelling of the pyrolysis and oxidation of large hydrocarbon molecules is very complex, both for the huge number of elementary reactions involved and for the number of intermediate species required for describing successive reactions. To reduce this complexity, a proper lumping approach, with extensive use of analogy rules, is adopted. This detailed kinetic mechanism is then used to derive reduced kinetic mechanisms, capable of describing the chemistry of surrogate fuel mixtures for jet-fuels inside a CFD simulation. Surrogate mixtures are well defined mixtures of a limited number of reference components, usefully applied to mimic the behaviour of real fuels in respect of particular investigation target, such as chemical properties include the right proportion of aromatics, naphthenes, and paraffines [2]. Recently Dooley et al. [3] proposed mixtures of n-decane, iso-octane, toluene, cyclohexane and methyl-cyclohexane were considered to emulate the combustion properties of an actual aviation fuel, POSF 4658 (see Table 1).

Table 1. Surrogates for jet fuel POSF 4658 [3]

Mole fraction	Surr_1	Surr_2	Surr_3
n-decane	0.4267	0.482	0.422
iso-octane	0.3302	0.175	0.174
Toluene	0.2431	0.178	0.179
Cyclohexane	-	0.165	-
Methyl-Cyclohexane	-	-	0.225

The chemical reactivity and auto-ignition properties of stoichiometric mixtures in air of POSF 4658, and the POSF 4658 surrogate were investigated in the following systems:

(1) A variable pressure flow reactor at 12.5 atm and 500–1000 K, with 0.3% C for both mixtures.

(2) A shock tube at 674–1222 K and pressures close to 20 atm.

(3) A rapid compression machine at 645–714 K at pressures close to 20 atm.

Finally, the strained extinction limit of diffusion flames were evaluated for measuring the high temperature reactivity and the kinetic-diffusion coupling of actual fuel and surrogate. In this paper we analyze and compare the predictions of the kinetic scheme with some of the available experimental measurements, including the recent n-dodecane shock tube experiments of Davidson et al [4] and the extinction experiments of Humer et al [5].

Figure 1 shows the comparisons between model predictions and experimental measurements for POSF 4658 surrogate. A very accurate agreement in the whole range of conditions can be observed. The ignition behavior of both POSF 4658 and its surrogate was also studied at pressures of ~20 atm and shock temperatures of 650-1200 K.

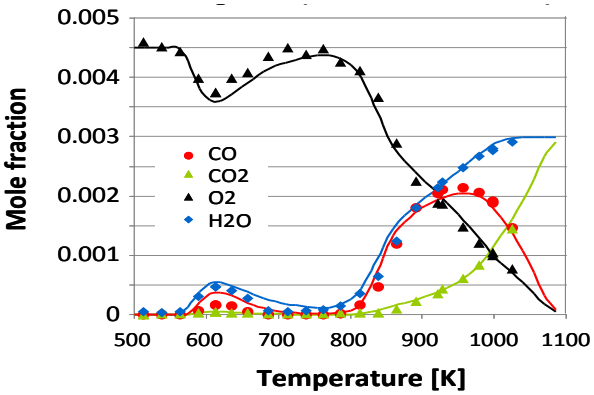

Figure 1. Flow reactor oxidation data for conditions of 12.5 atm and s = 1.8 s, for POSF 4658 surrogate (symbols) [3] and POLIMI kinetic model (lines).

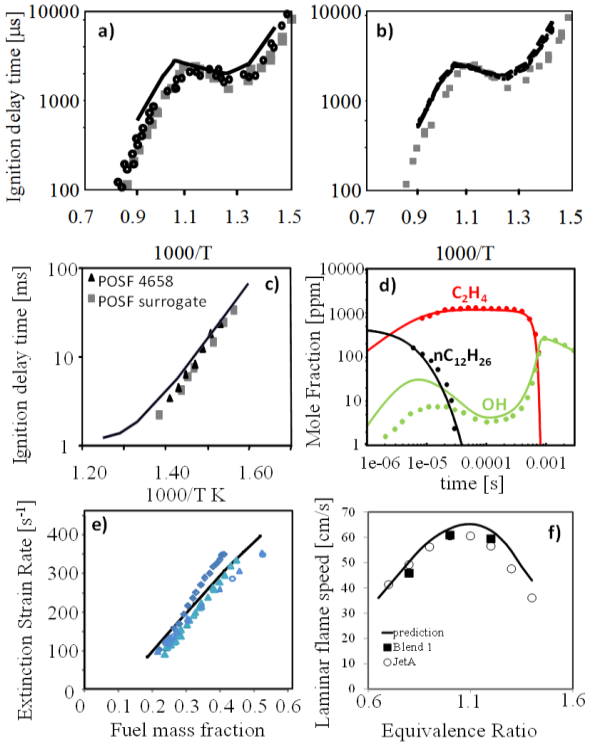

Figure 2. Panel a) Ignition delay times [4] for POSF 4658 (circles), its surrogate (squares) and predictions at 20 atm (line). Panel b) Ignition delay times for POSF 4658 surrogate (symbols) [3] and predictions at 20 atm (lines). Panel c) RCM measurements [3] and simulations. Ignition delay times for POSF 4658 16.3–24.8 atm (triangles), POSF 4658 surrogate 17.7–22.9 atm (squares) and model simulation (line). Panel d): Species time-histories. Points: experiments [4]. Lines: simulations. Initial reflected shock conditions: 1410 K, 2.37 atm, 457 ppm n-dodecane, 7577 ppm O_2/Ar. Panel e) Extinction Strain rates for counter flow diffusion flames at 1 atm. POSF 4658 (triangles), POSF 4658 surrogate (diamonds) Jet-A (empty triangles)

[4] and JP8 (empty circles) data [5], POSF 4658 surrogate simulation (line). Panel f) Predicted and measured [6] flame speed of JetA and surrogate kerosene blend (n-decane (82%), methylcyclohexane (8%), toluene (10%)) at Tin=400 K.

Figure 2 shows the agreement between the ignition delay times of POSF 4658 and its surrogate, then also shows that predicted ignitions of surrogate fairly agree with the measurements. Figure 2d shows the comparison between model predictions and experimental data in the Stanford shock tube device.n-decane measurements are not available, therefore the comparison is made using measurements for n-dodecane, which is also a component of several jet fuels surrogates [3]. It is possible to observe that not only the fuel consumption is well predicted by the model but also the formation of OH radical and ethylene is in very good agreement with the experimental data. Figure 2e shows the comparison between model predictions and extinction experimental data in a counterflow flames [3],[5]. It is possible to observe that the model is in general able to correctly predict the extinction strain rates at different fuel/N_2 ratios. Finally, Figure 2f shows a comparison with laminar flame speed of Jet-A and a surrogate kerosene blend [6].

2.2. Kinetic Post-Processing of an industrial combustor

Figure 3 shows the structure of the KPPSMOKE approach, which combines a CFD simulation followed by a kinetic post processing phase. The huge number of compounds and reactions contained in detailed kinetic mechanism prevents its direct use in CFD codes. Thus the kinetic model is automatically reduced to a limited number of species and reactions, with an eventual optimization of the proposed simplified kinetics [7]. The fluidynamic simulation with this reduced mechanism can be then run to evaluate the temperature and velocity profiles inside the combustion chamber. A detailed mechanism is adopted to evaluate the formation of pollutants in a postprocessing phase [1].

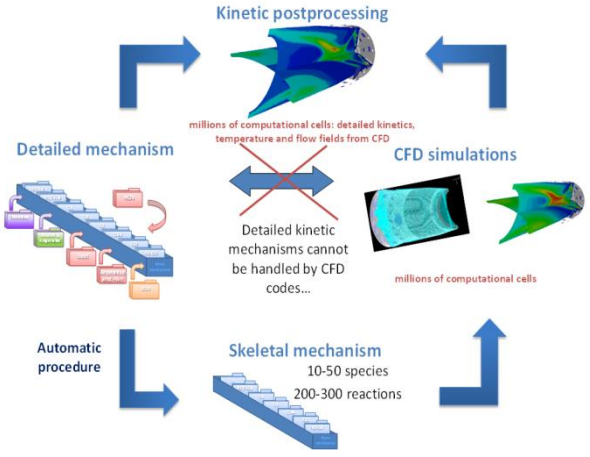

Figure 3. Use of detailed and reduced kinetics in CFD/KPPSMOKE simulations in the EMICOPER project [8],[9].

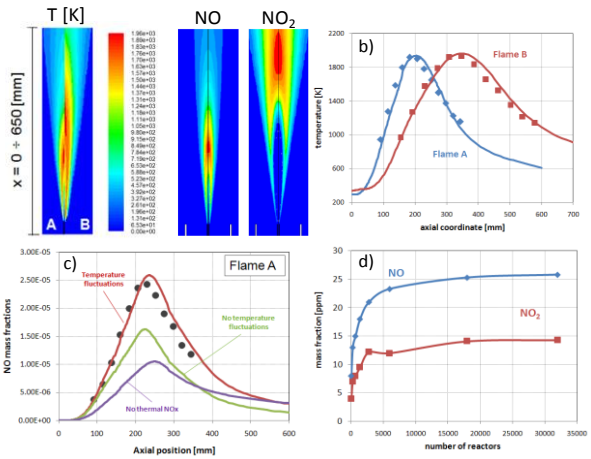

Figure 4. Temperature profiles along the axis for flame A and B [9] . Panel c) Comparison with measured NO axial profiles. The red lines is the KPPSMOKE results obtained considering the effects of temperature fluctuation on reaction rates [1]; the green line neglecting the temperature fluctuations; the purple line was calculated neglecting the thermal NOx mechanism.

Specific numerical algorithms were developed and adopted to improve robustness and efficiency of the solution. The overall procedure is described in detail in ref [1]. Local and global solutions are used and that Newton's method is combined to a time stepping algorithm. KPPSMOKE is also strongly parallelized [1] during both the local and global solutions and this allows to handle detailed schemes with a quite fine mesh.

Figure 4 shows an example of comparison with literature experimental data [10]. In particular, there is a good agreement for both temperature and NO profiles along the axis of the jet flame. The figure also shows the effect of temperature fluctuations on NO formation and that the thermal mechanism accounts for about half of the NO formed. Other similar comparisons can be found in [11],[12].

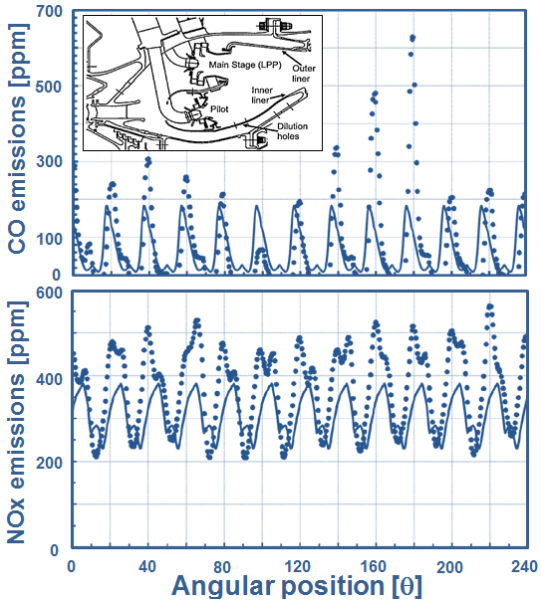

Figure 5. Aircraft combustor: outlet CO and NOx mole

fraction profile as predicted by KPPSMOKE (lines) vs. measurements (symbols) along the radial coordinate [1],[13].

Finally, the performance of this tool is analyzed through the comparison with an aircraft combustor [13] (~330000 cells), which is discussed in detail by [13] and [1]. The CFD domain is a periodic angular sector of 20 deg that includes the pilot and the main injector (Figure 5). Also in this case a good agreement with measured CO and NOx emissions is observed.

2.3. Engine characterization through literature data

The RR-Allison Model 250, which is a highly successful turbo-shaft engine family, has been studied in detail during the EMICOPTER project [8],[9]. This model propels a large number of helicopters (including the Agusta A109 and PZL SW-4). The Rolls-Royce Model 250-C20B Turboshaft Gas Turbine consists of a six stage axial compressor, a single stage centrifugal compressor, a single combustion chamber, a two-stage gas generator turbine, and a two-stage power turbine. The single-can combustion liner is shown in Figure 6.

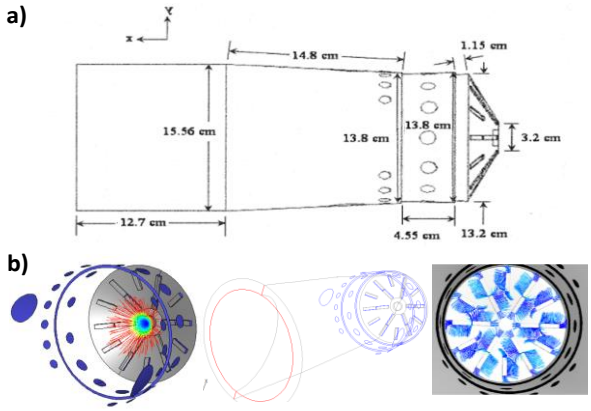

Figure 6. Panel a) RR-Allison 250 engine combustion chamber geometry (adapted from [14]). Panel b) spray patterns and droplet temperature. CFD geometry and simulation with predicted pathlines of the swirled flow.

This paragraph summarizes the available relevant information available in published articles and conference papers on the RR engine 250-C20B and its corresponding military version T63A-720. Similarly, also the C18 version (T63-700) are studied in the literature. The information contained in this paragraph are the result of an extensive and careful literature survey [15]-[22]. Thanks to this literature analysis it was possible to almost completely characterize the boundary conditions of the combustor for the different power settings, in terms of fuel and air flow rates, air pressure, temperature and air distribution. On the basis of the available information, a series of CFD simulations were performed to characterize the temperature and flow fields. The comparison with the available experimental measurements is quite satisfactory and allowed to apply the KPPSMOKE to evaluate the emissions. Table 2 summarizes some of the operating and boundary conditions of the test cases studied. SHP indicates the Shaft horsepower, i.e. the power delivered to the propeller shaft. Engine data of the PZL-SW4 helicopter were found in good agreement with the results of the literature analysis. Nevertheless, in Figure 7 it is possible to observe that the fuel flow rates adopted in the EMICOPTER project, which are mostly based on the values reported by Golden et al [20], are lower than the actual values measured by other authors and also during the flight tests, but only at high power conditions. This is an important point, because the data [20] implicitly assume a higher thermal efficiency of the engine at high power conditions, which is not completely consistent with the measured data on the SW4.

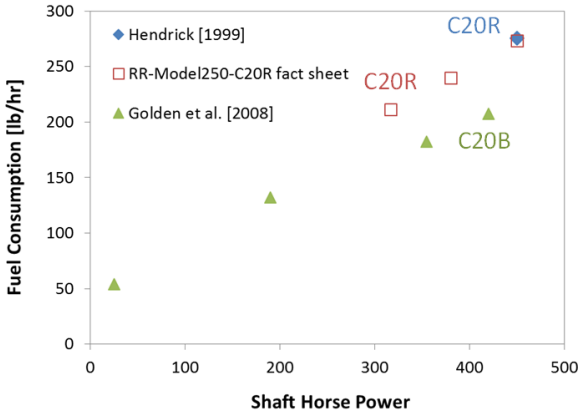

Figure 7. Comparison between fuel flow rates measured by different authors [15],[20],[22].

Table 2. RR250-C20B engine operating conditions

	Take off [14],[15]	Idle [20]
Airflow Rate [kg/s]	1.733	0.73
Fuel Flow rate [kg/s]	0.035	0.0068
Air Fuel Ratio (AFR)	49.87	106.7
Power [SHP]	450	25
Compressor exit T [K]	577	410
Compressor exit P [atm]	7.895	2.5
Combustor exit T [K]	1350	850
Combustor exit P [atm]	7.658	2.5

Figure 8 shows a comparison between experimental data and model predictions obtained using the CFD code Ansys-Fluent. The comparison shows that the model is able to correctly characterize the combustor exit temperature as a function of the fuel flow rate (engine power). This means that the boundary conditions are correctly characterized both in terms of air flow rates, fuel flow rate, temperature and pressure. It is important to observe that, as expected, the output temperature is not sensitive to the combustion model used.

The predicted results are obtained using a 1-step model [23] for kerosene and the flamelets approach using a skeletal kinetic mechanism and the Aachen surrogate [24] to describe the kerosene composition. The Hendrick et al [15] data refer to a RR-C20R engine, while Golden et al. [20] data refer to a RR-C20B model

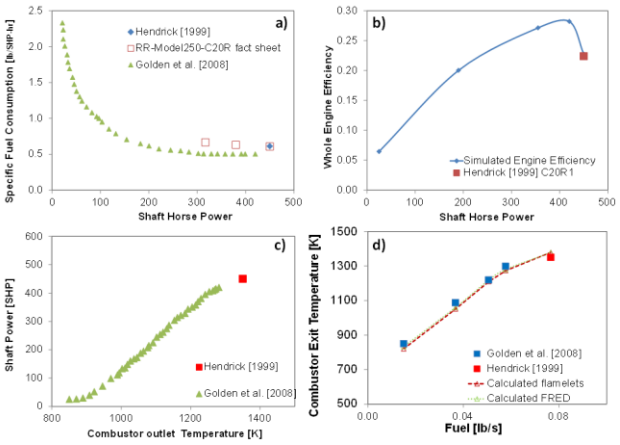

Figure 8. a) Specific fuel consumption as a function of the SHP. Data are taken from [15],[20],[22]. b) Calculated engine efficiency. The engine efficiency is calculated using the fuel flow rate and the SHP values taken from Golden et al. [20] and assuming a ΔHcomb=43000 kJ/kg. The SHP=450 refers to the 250-C20R1 engine of Hendrick et al. [15]. c) Variation of the Shaft Power with the combustor outlet temperature [15],[20]. d) Predicted and measured ([15],[20]) combustor exit temperature as a function of the fuel flow rate.

3. DEVELOPMENT OF A METHODOLOGY FOR EMISSION EXPERIMENTAL VALIDATION

MAEM-RO is a dedicated Clean Sky GRC-5 project aimed at developing a methodology for in-flight measurement of helicopter engines emissions.

3.1. Requirements for measurement system

In order to design a complete flue gas measurement system for flight tests many requirements have to be taken into account:

- system has to be robust enough to stand with helicopter vibrations without interfering with measurement accuracy and **flight safety**;
- it has to be not too much demanding from power point of view;
- capability of automatic operation, in order to avoid expert presence during flight;
- need of auxiliary equipments has to be reduced as much as possible.

These constraints required a deep study for designing each component and the whole system integration can be divided in several tasks:

Design of probe
The suction probe has to assure homogeneity in sampled gas for accurate measurements, and it must be robust to stand with gas high temperatures and engine vibrations. It has to be intrusive as small as possible, avoiding interference with engine performance and flight safety; that means suction probe should be designed as small as possible, but big enough to sample the right gas flow rate.

Sampling line
In case of HC measurements, it is necessary to avoid condensation of water vapor which causes reaction with hydrocarbons to be measured: heated sample line should be used. Its requirements have to be compatible with:

- power supply available on helicopter;
- external air temperature and pressure;
- installation path available from sampling probe to the helicopter cabin, where analyzers are supposed to be installed.

For those reasons sampling line has to be properly designed to take into account mentioned constrains.

Auxiliaries and flue gas conditioning
To work properly and for accurate measurements, flue gas analyzers require a flow rate control system with pump and filters to remove particles or dust. Components must be light and low-power demanding. Centro Combustione Ambiente specialists have designed the conditioning system, purchasing standards components but with operating features suitable for flight tests on helicopters.

Analyzers
On the market there are many flue gas analyzers, for example compact multi species analyzers, single species analyzers, based on NDIR principle (for CO, CO_2, NO_x, SO_2), chemiluminescence principle (for NO_x), FT-IR etc. Most of them can be considered at the state of art for this kind of equipment, but usually they have different requirements during operation. For example most of analyzers use optic measuring principle that is sensitive to vibrations. These requirements have to be compatible with helicopter flight conditions while measurements have to be accurate as much as possible. Centro Combustione Ambiente engineers have designed the integration of analyzers in the system taking into account all those constrains, choosing analyzers as more "standard" as possible to keep cost reasonably low, avoiding expensive and not well proofed equipment. Moreover anti vibration mounts will be adopted during flight tests.

Another important requirement is the response time of meters: even if only steady state measurements are meaningful, for aeronautic field steady states can be shorter than, e.g., power plants steady state. For this reason fast response analyzers should be adopted, with response time compatible with typical time of helicopter operation, like climb time.

3.1.1. Analyzers

For the flight measurement campaign, the analyzer Gasmet DX-4000 FT-IR was chosen, which is able to measure several components in about 1 second:

- SO_2
- CO
- CO_2
- NO
- NO_2
- N_2O
- HCl
- H_2O
- HF
- CH_4
- C_3H_8 (n-propane)
- C_6H_{14} (n hexane)
- HCOH (formaldehyde)
- O_2 measurement with ZnO sensor

This analyzer meets all the requirements for flight test.

Vibration issue
Vibration level in helicopter cabin during flight missions is one of the most important issue. Performances of Gasmet DX-4000 analyzer, equipped with a vibration isolator

system, have been investigated during vibration tests (Figure 9).

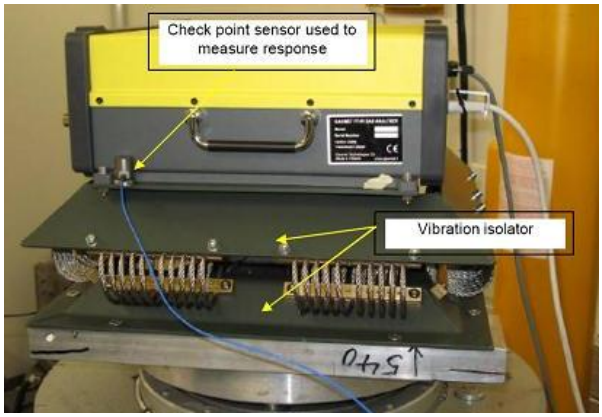

Figure 9. Analyzer under vibration tests

These tests show that this configuration is suitable for operations with typical helicopter vibration.

Weight issue
The complete set up for Gasmet analyzer for proper operations is composed by:

1. sampling probe (to be connected to sampling probe in the stack);
2. heated sample lines (n°2)
3. sampling unit;
4. analyzer;
5. notebook.

The sampling unit is used for:

a. extracting hot and wet gas emissions and removing particles
b. holding fine particle filter heated to 180 °C
c. carrying sample pump heated to 180°C and sample flow gas ~ 4 l/min
d. holding Automatic zero gas valve for test and calibration
e. holding temperature controllers for two heated lines (9 + 1 m maximum)
f. holding O_2 measurement with zirconium oxide sensor

Adopting 3+0,5 m heated lines the weight of the complete equipment is about 32 kg. The selected one is the lightest solution cabable of meeting all the performance requirements

Power request issue
Electrical power requirements of the installed system must be compliamt with the limited power available on board. Adopting a 3+0.5 m low power heated line the whole power consumption is 910 W @ 220 V_{ac}, which is compatible with the on-board power availability.

Automatic operation issue
After start up Gasmet analyzer is capable of automatic operation, fundamental to avoid the presence of a measurement specialist on board.

3.1.2. Sampling probe

The role of suction probe in the measurement chain is to assure homogeneity in sampled gas for accurate measurements.

The ARP1256B accepted system layout for continuous sampling and measurement of gaseous emission from aircraft turbine engines in shown in Figure 10. The sampling plane shall be as close to the engine exhaust nozzle exit plane as permitted by considerations of engine performance but in any case shall be within 0.5 nozzle diameter of the exit plane. Anyway this sampling procedure is definitely inappropriate for flight tests, first of all for flight safety reasons, moreover dilution effect of air on flue gases is dependent on probe tip position.

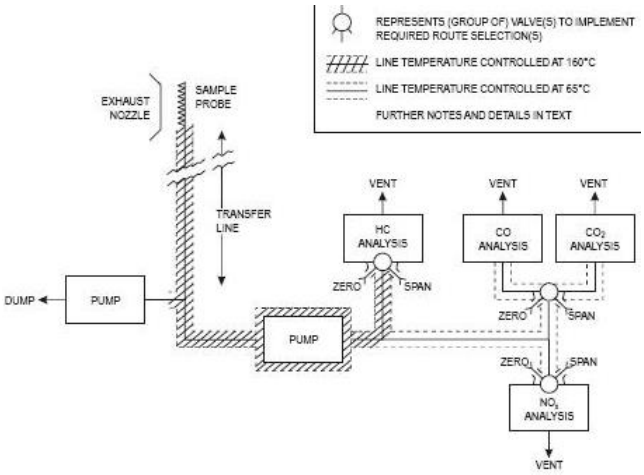

Figure 10. System layout for continuous sampling and measurement of gaseous emission from aircraft turbine engines.

In stationary gas turbines flue gases are sampled at the stack and the Italian UNI 10169-2001, partially derived by international ISO 10780-1994, prescribes suction probe systems and installations according to flue stack shapes. Due to size and shapes issues not all the requirements dictated by the international standards can be satisfied on helicopter stack. The stack cross section of the probe, installed in the left stack of the helicopter has been divided in three equivalent areas.

The sampling probe has been built in AISI 304 stainless steel, taking into account the maximum temperature of flue gas coming out from engine turbine. AISI304 has good oxidation resistance in intermittent service to 870°C and in continuous service to 925°C, well above the temperature of flue gases. Five 3mm sampling points have been drilled on the probe.

The sampling probe has been welded on the stack, as shown in Figure 11, according to qualified TIG (tungsten inert gas) welding procedures.

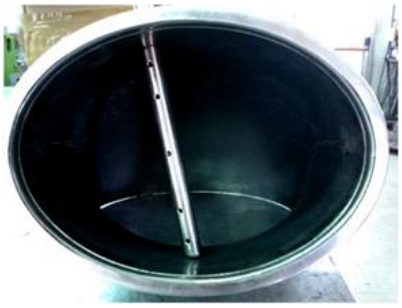

Figure 11. The sampling probe welded on the stack

3.2. On-board installation

In January 2013, the analyzer system has been succesfully installed on SW-4 helicopter in Swidnik (Poland), Figure 12. Both analyzer and sampling unit have been mounted on anti vibration plates in order to dampen vibration in cabin as much as possible.

Figure 12. Analyzer system installed on board of helicopter

3.3. Ground test

In order to check installation and integration of devices on helicopter a preliminary ground test campaign has been carried out after installation on board. The ground test has been performed in severe weather condition with snow and -2 Celsius air temperature.

With the purpose of understanding the minimum time required to reach a steady value of flue gases concentrations , a preliminary ground test has been carried out.

Following the preliminary ground tests results, it has been agreed with the flight test crew to maintain each flight condition stabilized for a minimum time of two minutes (see Table 3).

3.4. Flight test campaign

The purpose of the experimental campaign was to measure gaseous emissions and main engine parameters during ground and flight tests, so as to write up a database of the pollutant emissions in different operating conditions of the PZL SW-4 helicopter to be used to validate the numerical combustion model. The test sequence includes a check flight (No. 1733), a steady-states flight (No. 1734), a baseline mission profile (No. 1735) and an alternative mission profile (No. 1736).

Table 3. Steady-state flight conditions (No. 1734).

Cond. #	Flight condition	Marker No.	OAT [°C]	Baro alt. [m]	V. speed [m/s]
1	hover IGE	11	20.7	163.3	
2	level flight	15	17.0	297.5	
3	level flight	17	17.6	310.4	
4	level flight	19	17.5	300.6	
5	level flight	21	17.8	266.9	
6	level flight	23	17.6	291.8	
7	climb	25	17.2	452.0	2.77
8	level flight	27	14.1	1210.5	
9	level flight	29	14.1	1212.9	
10	level flight	31	14.6	1210.2	
11	level flight	33	14.5	1203.3	
12	level flight	35	14.1	1212.7	
13	MCP	37	11.9	1738.8	3.6
14	level flight	39	6.0	2413.5	
15	level flight	41	6.3	2417.4	
16	level flight	43	8.9	2422.5	
17	level flight	45	9.3	2446.3	
18	descent	47	7.4	2258.2	-2.23
19	descent	49	11.2	1697.4	-4.37
20	descent	51	16.3	744.6	-4.35
21	climb	53	17.1	496.0	2.5
22	descent	55	15.8	711.1	-2.15
23	climb	57	16.8	669.2	4.67
24	descent	59	16.2	678.4	-1.98
25	climb	61	17.1	682.2	5.19
26	descent	63	17.1	528.8	-4.49

The mission profiles (Flights No. 1735 and 1736) will be described in section 5.

3.5. Predictive tool validation

The results from the ground and flight test campaign were used to populate a database for predictive tool validation.

Figure 13 shows a comparison between measured and predicted NOx emissions from the RR-Allison C20B engine. Model predictions, obtained using the parallel version of the KPPSMOKE code described in this paper, are presented for the fluid dynamics simulations performed using a simple 1-step kinetics [23] (FR-ED) and the skeletal mechanism (flamelets). As expected, the simple chemistry leads to an overestimation of the temperature peaks, and therefore the NOx emissions are overestimated, due to the thermal NOx mechanism. On the contrary, the KPPSMOKE predictions based on the CFD simulations performed adopting detailed chemistry well agree with the measurement. It is worth noting that the model is able to reproduce the trend of NOx emissions as a function of the combustor outlet temperature, but also air flow rate and shaft power. More importantly, no tuning parameters are used to calculate the emissions. The approach (CFD+KPPSMOKE) is fully predictive and the quality of the results largely depends on the accuracy of the models adopted inside the CFD simulation, especially for the turbulence-chemistry interactions and the spray characterization. Nevertheless, also turbulence model play a role. In fact, Figure 13 also shows the effect of the turbulence model used. The standard k-ε model (SKE) tends to predict slightly higher flame temperature peaks than the realizable k-ε (RKE) model does. As a consequence, the predicted NOx emissions based on the standard k-ε are closer to the experimental results. It is important to observe that the KPPSMOKE simulations partially fail to predict the emissions for the low engine power case. This deviation can be, at least partially, due to the uncertainty associated to the characterization of the

fuel spray. The spray angle and droplets diameter are not known for the low fuel flow rates (low engine power). We assumed the values of Hendrick [15] measured at high power conditions.

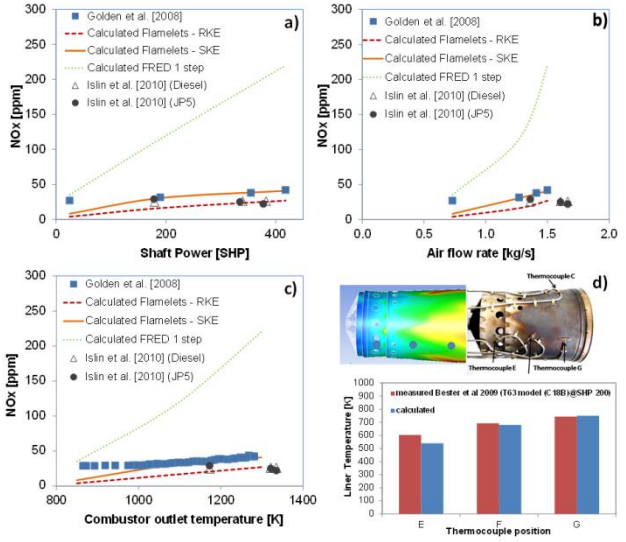

Figure 13. Panels a-c) Calculated NOx emissions. Predictions are based on CFD simulations performed using global 1-step kinetics, flamelets approach and k-ε turbulence models. Measurements are from [19],[20]. Panel d) Predicted temperature distribution in the liner walls (left) and thermocouple placement on an instrumented T63 (250-C18B model) liner [18].

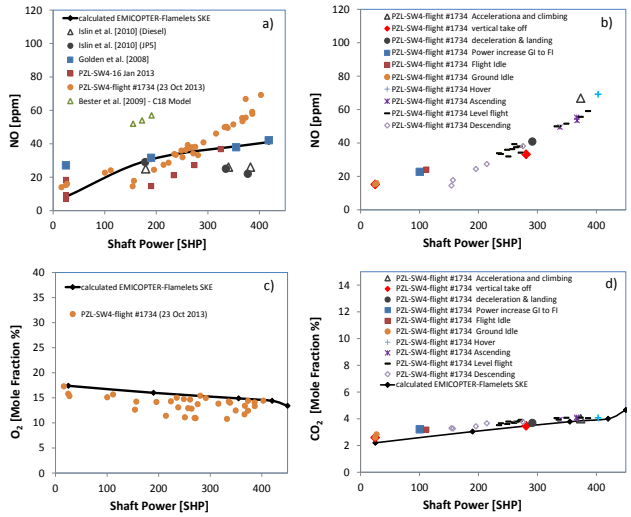

Figure 14. Panel a) Comparison between measured and calculated NO emissions, for the ground test and flight #1734. NOx predictions are based on post-processing of CFD simulations and were performed in the EMICOPTER project [8],[9]. Panel b) NO emissions from PZL-SW4 during the different phases of flight #1734. Panel c) O_2 mole fraction (%) in the flue gases. Panel d) Detailed analysis of CO_2 emissions.

Figure 14 shows a comparison between model predictions, literature data and the corresponding measurements obtained during the experimental campaign on the SW4 helicopter. It is possible to observe that the amount of NO emitted from the SW4 helicopter reasonably agrees with the predictions and with the other measurements. Only the data of Bester et al. [18] seem significantly higher than the other dataset, but that these values are measured using a RR-250-C18 model, which is similar, but not the same, to the C20 used by the other authors and installed onboard the SW4 model. A second comment can be made. At high power conditions, the predicted NO values seem more in line with the experimental data of Golden et al [20] while the emissions of the SW4 engine are higher. This deviation is quite small and partially lies within the experimental uncertainties, but it is important to notice that the EMICOPTER simulations were performed assuming the fuel flow rate presented by Golden at al. [20] and already discussed in Figure 7. These data refer to a RR-250-C20B model. The air flow rate of [20] is in very good agreement with the SW4 engine data, while at high power conditions the fuel flow is lower. This means that at high power conditions there is a higher Air/Fuel ratio which could explain the lower emissions measured by Golden et al. [20]. The effect of a slightly higher A/F ratio explains the tendency to overestimate the amount of O_2 in the flue gases (see Panel c)). Panels b) and d) of Figure 14 present the effect of the different flight phases on the emissions of NO and CO_2. As expected, the emissions of CO_2 are well correlated with the engine power, and do not significantly depend on the flight phase but mostly on the engine power needed for the particular flight phase. The same conclusion holds in respect of the NO emissions.

4. ESTIMATION OF PZL SW-4 EMISSION INDICES

The previous results can be compared to other experimental measurements from literature. Rindlisbacher [25] reported the results of an experimental campaign on the emissions of helicopter engines and suggested simple mathematical functions for correlating helicopter engine emission factors with SHP. Figure 15 shows a comparison between the measurements obtained using the PZL-SW4 helicopter with the corresponding measured emission indices from the literature [25]. Similarly to what suggested by Rindlisbacher, simple power law correlations based on the SHP are proposed for the different emission indices for the PZL-SW4 helicopter. The emission indices correlate the amount of grams of a pollutant species divided by the kg of fuel consumed, for the different engine power conditions considered. For this reason, it is possible to observe that the EINOx (g of NOx defined in terms of equivalent NO_2 per kg of fuel) increases with the SHP because of the higher temperature inside the combustion chamber. The value of EINOx of the PZL helicopter are in line with the measured values available in the literature. Nevertheless, it is important to notice that there is an evident, unexpected and anomalous amount of EINOx at very low power conditions (Idle).

Figure 15b shows the emission index for NO (i.e., considering only the EINOx based on measured NO emissions and neglecting the contribution of the measured NO_2). In this case it is possible to observe that the results are more consistent also at low power conditions. Moreover, the EMICOPTER project simulations are in good agreement with the NO experimental data, meaning

that the amount of NO_2 is responsible for the observed deviation between measured and calculated total EINOx and for the anomalous behavior at low power conditions.

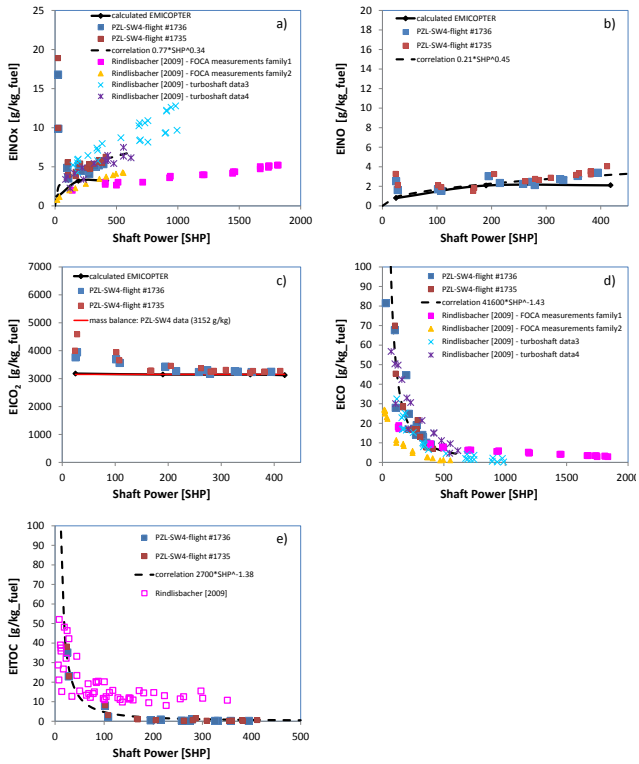

Figure 15. Comparison between measured and calculated Emission Indices for different pollutants.

It is also possible to observe that the NOx emissions are largely influenced by the engine characteristics in terms of combustion technology, geometry etc. For example, for an engine power of 400 SHP, the EINOX span between 4 and 8, with the PZL EINOx=6.

The PZL emission index for NOx can be correlated with the following function: $0.77 \times SHP^{0.34}$. Since the low power conditions data are anomalous, they were not considered for calculating this correlation.

Panel c) of Figure 15 shows a comparison for the emission index of CO_2. This value should be mostly constant, because CO_2 emissions directly depend on the fuel consumption. The effect of CO and unburned hydrocarbons, which could in principle reduce the measured $EICO_2$, is negligible since the CO_2 mole fraction in the flue gases is orders of magnitude larger than the typical emissions of CO and unburned hydrocarbons. The predictions of the EMICOPTER project are in good agreement with the $EICO_2$ calculated on the basis of the actual fuel composition: $EICO_2$=3152 g/kg_fuel.

Panel d) shows the same comparison for CO. Also in this case the measured values for the PZL helicopter are consistent with the other available literature results, also at low power conditions were CO emissions are typically very high form gas turbine engines. The PZL-SW4 emission index for CO can be calculated as $41600 \times SHP^{-1.43}$. A similar results is obtained for the Total Organic Carbon (TOC), which is mostly emitted at low power conditions. $EITOC=2700 \times SHP^{-1.38}$.

5. MISSION PROFILE OPTIMIZATION

5.1. SW-4 flight data and comparison with FOCA indices

As a public benchmark of pollutant estimation, the results obtained in GRC5 TP10 activities were compared with those from the Swiss Federal Office for Civil Aviation (FOCA) [15]. The engine models used by FOCA arise from technical investigations and measurements aimed at updating the Swiss civil aviation emission inventory, improving the quality of the data contained therein. Still, the validity of the models behind the updated FOCA estimations is clearly stated in a specific disclaimer [15]:

"Caution: Despite the degree of detail in the FOCA method, which allows estimating emissions for individual helicopters, the practitioner must be aware of the fact that individual helicopter engine emissions characteristics are not taken into account to produce the results. A result gained with the estimation functions of this methodology and a result based on the knowledge of specific individual engine data may differ by a factor of 2 or more. For the same reason, it is not appropriate to use the method to compare helicopter emissions of different helicopters of similar size."

Indeed, the comparison of typical TP10 results against estimates made using FOCA engine models shows an average error higher than 15% on the predicted fuel flow, which generates by itself a proportional error in CO_2 emission estimations.

The Fuel Flow difference shown in Figure 16 is calculated as reported in the equation below, so negative values mean that TP10 estimates are lower than FOCA ones:

(1) (GRC5_TP10 - FOCA) / FOCA [%]

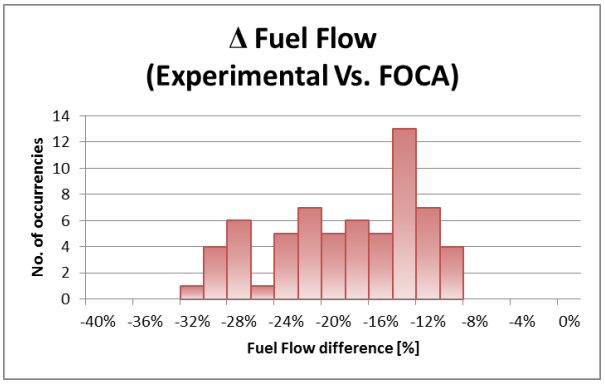

Figure 16. Fuel Flow difference between TP10 and FOCA estimated values, expressed as percentage of the FOCA values.

Regarding the other pollutant specimens, the difference between the FOCA estimates and the TP10 results falls in the ranges shown in the following table and charts.

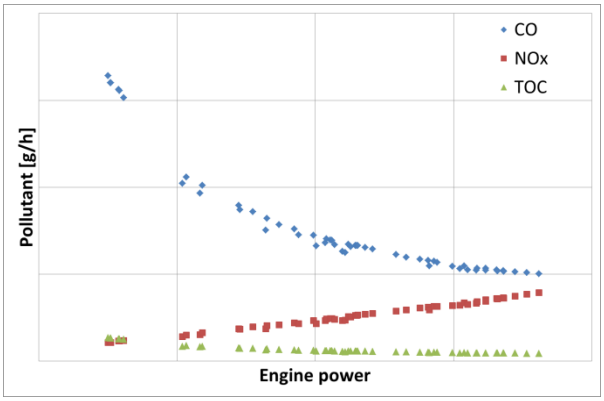

Figure 17. PZL SW-4 CO, NOx, TOC emissions as a function of engine power.

Table 4. Estimated pollutant emissions comparison (TP10 Vs. FOCA). Negative values mean that TP10 estimates are lower than FOCA ones.

	Δ CO [%]	Δ NOx [%]	Δ TOC [%]
Max	131%	54%	-9%
Min	-4%	-21%	-31%
Mean	16%	-8%	-18%

As per the Fuel Flow, the values of pollutant emission difference shown in Table 4 are calculated following equation (1).

For converting unburnt fuel (HC, Hydrocarbon, also reported as THC, Total Hydrocarbon) to TOG (Total Organic Gases, also reported as TOC), we used the following relation from Ref. [16]:

Equation No. 3:

Conversion to TOG

THC Emissions (kg) x TOG Conversion Factor = TOG (kg)

As shown in Table 4, the THC to TOG conversion factor is 1.16. Therefore, the amount of TOG emitted by the A320 aircraft in this example is an estimated 322.22 kg.

If not only the effect of FOCA fuel flow models as function of shaft power is considered, but also FOCA relations for pollutants in terms of power and fuel flow, the pollutant estimation accuracy is found in the range of 15-50% in the case of CO and NOx pollutant species, while for TOC (unburnt fuel) the estimation is typically inaccurate up to one order of magnitude.

As anticipated by FOCA itself, the not negligible differences which were presented above make evident that the accurate characterization of the specific helicopter performance and engine pollutant production is necessary not to under- or over-estimating environmental benefits.

5.2. SW-4 optimised mission

To extend the analysis of the performance and pollutant emission of the PZL SW-4 helicopter, two profiles of the same mission have been designed, estimated and flown.

Table 5. Mission profiles description.

#	1000ft flight	6000ft flight
1	Engine start-up	Engine start-up
2	Ground idle (GI)	Ground idle (GI)
3	GI → Flight Idle (FI)	GI → Flight Idle (FI)
4	FI	FI
5	Vertical take-off	Vertical take-off
6	Hover: HZ = (1÷1.5) m	Hover: HZ = (1÷1.5) m
7	Acceleration and ascending at constant maximum power to H=1000ft, NR=103%	Acceleration and ascending at constant maximum power to H=6000ft, NR=103%
8	Horizontal flight at V = 100 KIAS to target point (50 km from TO) H = 1000ft, NR=103%	Horizontal flight at V = 100 KIAS to target point (50 km from TO) H = 6000ft, NR=103%
9	N/A	Descent at V = 60 KIAS, H = (6000 → 1000) ft
10	Left turn: 7200. Roll 30°, V = 60 KIAS, H = 1000 ft	Left turn: 7200. Roll 30°, V = 60 KIAS, H = 1000 ft
11	Right turn: 7200. Roll -30°, V = 60 KIAS, H = 1000 ft	Right turn: 7200. Roll -30°, V = 60 KIAS, H = 1000 ft
12	N/A	Ascending at constant maximum power to H = 6000ft
13	Horizontal flight at V = 100 KIAS to TO location H = 1000ft	Horizontal flight at V = 100 KIAS to TO location H = 6000ft
14	N/A	Descent at V = 60 KIAS, H = (6000 → 1000) ft
15	Braking to hover	Braking to hover
16	Vertical landing	Vertical landing
17	GI, cooling, stop.	GI, cooling, stop.

The pollutant emission data presented in Table 6, are calculated integrating the values over the whole mission profiles, from take-off to landing. The comparison of the results in the two cases (cruise altitude 1000 ft and 6000 ft), shows that for such a short mission (50 km radius) the low altitude cruise is more efficient in terms of fuel consumption and pollutant emissions.

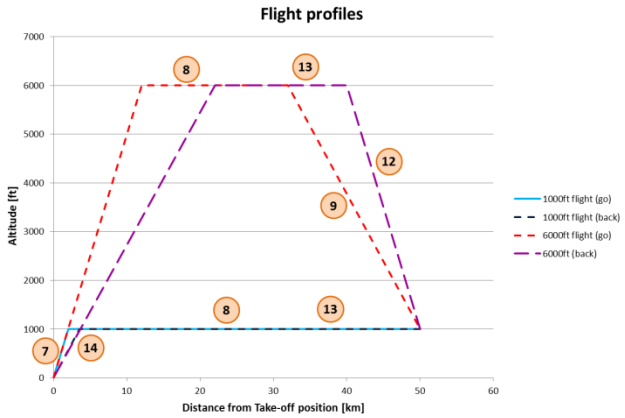

Figure 18. Mission profile schematics.

Table 6. Cumulative pollutant masses. Comparison over the whole mission (from Take-off to Landing) for different cruise altitudes (1000 ft and 6000 ft).

POLLUTANT SPECIES	6000 ft	1000 ft		difference [%]
CO_2	287.6	265.7	kg	-7.6%
CO	1.1	1.0	kg	-8.7%
NO	263.5	217.9	g	-17.3%
TOC	40.9	15.4	g	-62.3%
Fuel	*92.4*	*86.5*	*kg*	*-6.4%*

For the profile optimization activity, a mission aimed at the "Inspection of ground facility in specific range of T-O airfield" has been identified. For this kind of mission the fuel efficiency is highly beneficial.

The mission radius adopted is 300 km. Cruise speed has been set according to the Rotorcraft Flight Manual:

- VTAS1 = 185 km/h – velocity for the minimum fuel consumption in kg/km;
- VTAS2 = 115 km/h - velocity for the minimum fuel consumption in kg/h during climb, descent and turns.

Flight altitude has been selected after checking (on calculation basis) at which altitude fuel consumption would be the lowest. For this reason calculation of fuel consumption for six flight profiles has been performed.

After the calculations the following two profiles have been designated:

<u>Standard mission profile</u>

- Take – off on altitude H=300m
- cruise 300km on altitude = 300m
- VTAS=185km/h, 2 left turns and 2 right turns, 300km return, landing.

<u>Optimized mission profile</u>

- Take-off on altitude H = 300m
- climb up to 2000 m
- cruise to target point distant 300 km from take-off place
- descent to 300 m
- 2 left turns and 2 right turns
- climb up to H = 2040 m
- return cruise
- descent
- landing.

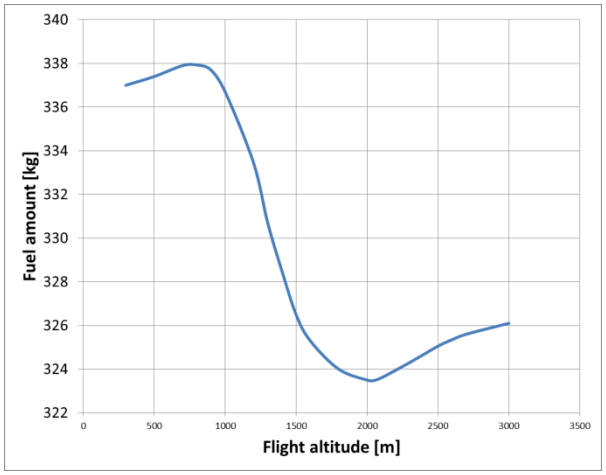

Figure 19. Whole mission fuel consumption, as a function of cruise altitude (mission radius 300km, ISA conditions).

Figure 19 shows that the cruise altitude which minimize the fuel consumption for the mission described (300 km radius) is 2040 m (6700 ft), allowing 14 kg fuel saving with respect to 300 m cruise altitude condition.

PZL performed also the estimation of the fuel saving trend as a function of the mission radius. The same mission analysis has been performed for two different altitudes (300 m and 2000 m), varying the mission radius.

As a baseline for this analysis, the following mission conditions have been considered:

- take – off at 300 m
- climb to cruise level
- cruise to mission target point
- descent from cruise level up to 300 m
- two left turns, two right turns at 300 m
- climb up to cruise level
- cruise to starting point
- descent from cruise level up to 300m
- landing
- ISA conditions
- mission radius: 100, 200, 300 km
- flight altitude: 300m and 2000 m
- velocity: 185km/h
- rate of climb, rate of descent and turns 115 km/h.

In order to verify whether a fuel saving is followed also by a reduction of the main pollutant species produced, the Emission Indices presented in section 4 have been used to estimate the pollutant emissions in the different missions analysed.

Flight parameters, fuel consumption and pollutant emissions are presented in the following Table 7, which shows the differences between low and high altitude cruise missions.

Table 7. Reduction of fuel consumption and pollutant emissions for a cruise altitude of 2000 m, with respect to 300 m baseline cruise altitude, as a function of mission radius. (Negative value means pollutant reduction

@2000m)

Radius [km]	Fuel, CO_2	CO	NOx	TOC
100	3%	25%	1%	24%
200	-2%	13%	-3%	12%
300	-4%	9%	-6%	8%

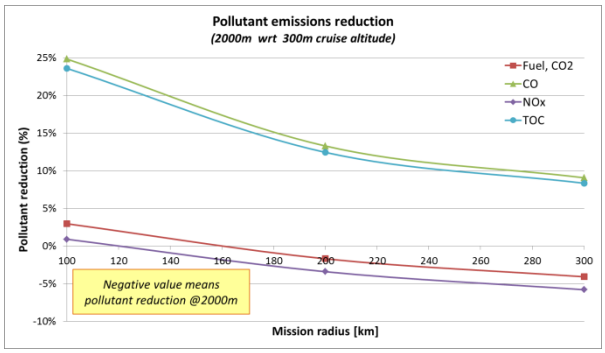

Figure 20. Reduction of fuel consumption and pollutant emissions for a cruise altitude of 2000 m, with respect to 300 m baseline cruise altitude, as a function of mission radius.

5.3. SW-4 mission optimization conclusions

The analyses presented in the previous section shows that there is a trade-off between low fuel consumption in high altitude cruise and the increased fuel consumption due to the longer climb phase.

Anyway, for missions with a radius greater than ca. 160 km, it's worth flying at 2000 m thanks to the higher cruise efficiency. For a mission radius of 300 km, the fuel saving in this kind of mission is about 4%.

The pollutant emissions trend follows the fuel consumption one, but with some differences:

- The high-altitude cruise is beneficial for NOx emission also for shorter missions (less than 150 km). This is due to the nonlinear dependence of the NOx generation from the shaft power: the higher NOx generation in the climb phase is compensated soon by the lower NOx production in cruise and in descend mode.
- The amount of both CO and TOC generated decreases with the cruise altitude, but the total amount of CO and TOC emitted is higher for a cruise altitude of 2000 m even in case of mission radius of 300 km.

However, from another point of view, a low-altitude mission profile (300 m) is slightly more productive, because it allows a reduction of the mission time of about 11 minutes.

5.4. Light Single Engine Helicopter generalisation

To support the estimates provided in the previous sections and extend their validity, AW performed a specific performance analysis task. The aim of the activity was confirm the trends found by PZL using the SW-4 experimental data and numerical models, employing the single engine AW helicopter model of the AW119.

In particular, for a given mission range, it has been found that the optimal cruise altitude minimizing the consumed fuel (or equivalently the produced CO_2) can be either high or low, depending on the mission range itself.

So, the interest is here to confirm the trade-off between cruise altitude and mission range with a different single-engined helicopter, estimating possible fuel reduction strategy and quantitative benefit.

This is the baseline mission considered:

- take–off;
- climb to cruise level;
- cruise;
- descent from cruise level;
- landing.

The following vehicle parameters have also been considered to construct the matrix of missions analyzed:

- ISA conditions;
- mission radius: 50, 75, 100, 125, 150 km;
- flight altitude: 2000, 4000, 6000, 8000 ft;
- velocity: best range speed;
- climb speed = 75 kts;
- descent speed = 115 kts.

Note in particular that dry weight and mission ranges have been chosen to simulate representative missions of the AW119, with an average required power level sufficiently high and coherent with the tests and results reported above for the SW-4.

Figure 21 shows indeed that, also for the AW119, longer missions have a distinctive benefit when the cruise is flown at higher altitude: for very long missions, the fuel (and CO_2) saving can reach 9%, with respect to an equivalent mission flown at lower level. This is the result of the more environmentally-efficient cruise phase at high altitude, which requires a small "investment" of energy (and fuel burnt) to bring the vehicle at that level.

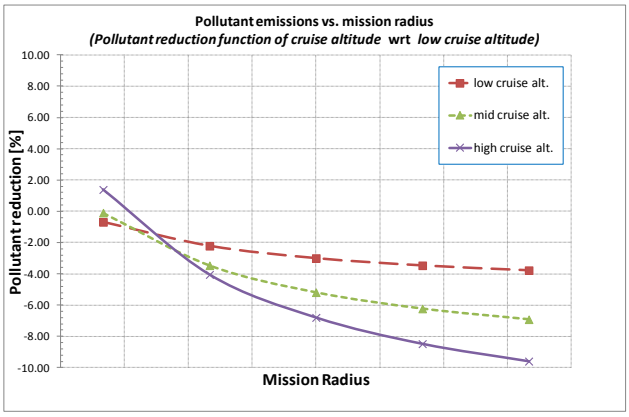

Figure 21. CO_2 reduction (in percentage) as function of mission radius for varying altitudes. Low-altitude cruise is best for short ranges, high altitude for longer ranges.

For shorter missions, the trend is inverted, as the additional fuel burnt to reach higher altitudes is not fully compensated by the saving in the cruise phase. Low-altitude cruise mission has in this case an advantage of roughly 1.5% over the high-altitude cruise mission.

Figure 22 and Figure 23 specifically show the mission profiles flown for each mission range, detailing the fuel consumption per unit km estimated in each situation.

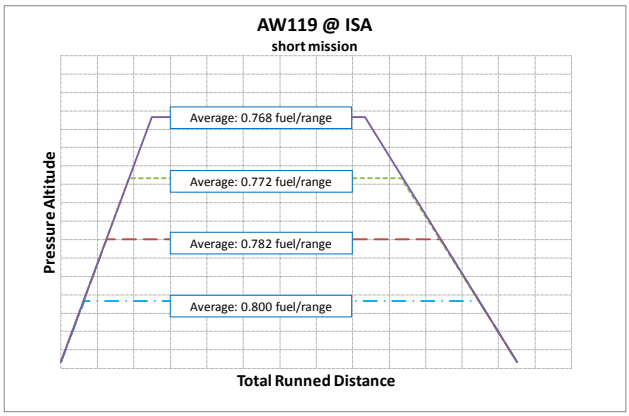

Figure 22. 50-km range mission profile, with indication of fuel consumption per unit mission radius for varying cruise altitudes.

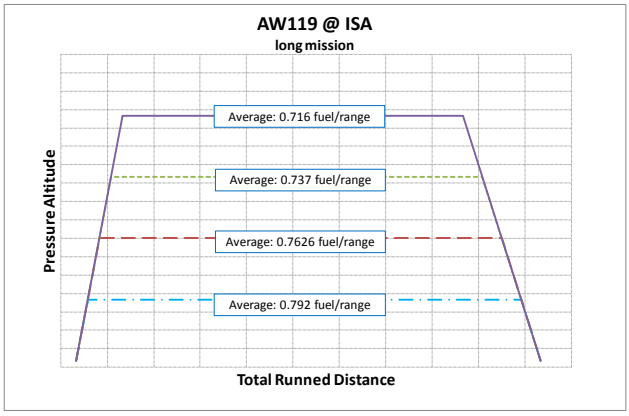

Figure 23. 150-km range mission profile, with indication of fuel consumption per unit mission radius for varying cruise altitudes.

5.5. Mission profile optimization – conclusions

The analysis shows that for a particular mission, parameters such as the altitude, flight velocity and helicopter take-off weight can be chosen in order to minimize the amount of fuel burnt, thus minimizing pollutant emissions.

Optimization of the mission parameters requires parallel analysis of power required with designated parameters, as well as engine fuel consumption and pollutant emission characteristics for the actual flight parameters. This requires both an accurate computational helicopter model and a comprehensive engine characterization, to properly simulate the behavior of these subcomponents. The ability to perform such optimization is confirmed by the analyses made for the designated missions.

In terms of mission fuel consumption, in the case of the PZL SW-4 the optimal flight altitude for the mission with a radius less than 80 nm is the altitude of 1000 ft; it is about 6000 ft for a radius greater than 80 nm. This result has been proven both by simulation and experimental flight.

Pollutant emission trends are correlated to the fuel consumption, with some distinctions:

- CO_2 production is directly connected to the fuel burnt, share the same minimization strategy and trade-offs;
- The high-altitude cruise is beneficial for NOx emission also for shorter missions (less than 150 km) with respect to fuel and CO_2. This is due to the nonlinear dependence of NOx generation on shaft power and fuel consumption;
- The additional amount of both CO and TOC for high-altitude cruise with respect to low-altitude cruise decreases with the mission range, but the total amount of CO and TOC emitted is higher for a cruise altitude of 2000 m even in case of mission radius of 300 km.

In terms of the duration of the mission, the best is the altitude of 1000 ft.

The trend “low-altitude cruise is CO_2-optimal for short range” and “high-altitude cruise is CO_2-optimal for long range” has been confirmed using an accurate performance model of the AW119, with a maximum fuel and CO_2 saving respectively of 1.5% and 9% for short range and long range.

6. CONCLUSIONS

The work described in the present paper was aimed to perform an extensive characterization of the SW-4 engine, the Rolls-Royce Allison 250-C20B. The characterization is based on an extensive and careful literature survey and on the experimental tests campaign which allowed also to develop a method for in-flight flue gas measurement.

On the basis of the available information, a series of CFD simulations has been performed to characterize temperature and flow fields of the gases inside the engine combustion chamber. The results of the above mentioned analyses have been compared with literature and experimental data, in terms of specific fuel consumption, air pressure and air temperature.

Since the comparison with the experimental measurements is quite satisfactory, it could be possible to apply the Kinetic Post Processor to evaluate the formation of different pollutant species.

The composition of PZL SW-4 engine exhaust gases have been analysed in terms of nitrogen oxide (NO), carbon dioxide (CO_2) oxygen (O_2) and water (H_2O).

It has been possible to observe that the measured pollutant gas emissions reasonably agree with the predictions. Only some of the literature data seem significantly higher than the other dataset, but it is worth nothing that these values were measured using a RR-250-C18 model, which is similar, but not the same, to the C20 used by the other authors and installed onboard the SW4 model.

Then, the predictive tool developed has been used for low-consumption mission profile optimization. The analysis shows that for a particular mission, parameters such as the altitude, flight velocity and helicopter take-off weight can be chosen in order to minimize the amount of fuel burnt, thus minimizing pollutant emissions.

Finally, some guidelines for mission profile optimization in terms of fuel consumption (and thus CO_2 generation), NOx emission and productivity has been derived for light single-engined helicopters.

7. ACKNOLEDGMENTS

This research was partially supported through the CleanSky Green Rotorcraft research project, under the grant agreement CSJU-GAM-GRC-2008-01.

8. REFERENCES

[1] A. Stagni, A. Cuoci., A. Frassoldati, T. Faravelli, E. Ranzi, A fully coupled, parallel approach for the post-processing of CFD data through reactor network analysis, Computers and Chemical Engineering 60 (2014) 197–212.

[2] Edwards, T., & Maurice, L. Q. (2001). Surrogate mixtures to represent complex aviation and rocket fuels. Journal of Propulsion and Power, 17(2), 461-466.

[3] Dooley S., S. H. Wona, M. Chaos, J. Heyne, Yiguang Ju, F. L. Dryer, K. Kumar, C-J. Sung, H. Wang, M. A. Oehlschlaeger, R. J. Santoro, T. A. Litzinger 'A jet fuel surrogate formulated by real fuel properties' Comb. Flame (2010) 157 (12):2333-2339.

[4] Davidson D.F., Hong, Z., Pilla, G.L., Farooq, A., Cook, R.D., Hansona, R.K., Multi-species time-history measurements during n-dodecane oxidation behind reflected shock waves, Proceedings of the Combustion Institute, 33(1):151-157 (2011).

[5] Humer, S., A. Frassoldati, S. Granata, T. Faravelli, E. Ranzi, R. Seiser , K. Seshadri 'Experimental and kinetic modeling study of combustion of JP-8, its surrogates and reference components in laminar nonpremixed flows' Proc. Comb. Institute 31 (2007) 393–400.

[6] B.M. Denman, J. D. Munzar, J. M. Bergthorson, An experimental and numerical study of the laminar flame speed of jet fuel surrogate blends, Proceedings of the ASME Turbo Expo 2012, paper GT2012-69917B.

[7] Stagni A., Cuoci A., Frassoldati A., Faravelli T., Ranzi E., "Lumping and reduction of detailed kinetic schemes: an effective coupling", Industrial & Engineering Chemistry Research, 2014, 53, 9004−9016 (2014).

[8] EMICOPTER project (CS-GA-2009-251798) final report (2013)

[9] Frassoldati, A., Cuoci, A., Faravelli, T., Ranzi, E., CFD simulation and emission estimation from helicopter engines, "Greener Aviation 2014: Clean Sky Breakthroughs and worldwide status", March 12th to 14th, 2014 , Brussels, Belgium

[10] Barlow, R.S., et al., Experiments on the scalar structure of turbulent CO/H2/N2 jet flames. Combustion and Flame, 2000. 120: p. 549-569.

[11] Cuoci, A., Frassoldati, A., Stagni, A., Faravelli, T., Ranzi, E., Buzzi-Ferraris, G., Numerical modeling of NOx formation in turbulent flames using a kinetic post-processing technique (2013) Energy and Fuels, 27 (2), pp. 1104-1122.

[12] Frassoldati, A., Cuoci, A., Faravelli, T., Ranzi, E., Colantuoni, S., Di Martino, P., Cinque, G., Kern, M., Marinov, S., Zarzalis, N., Da Costa, I., Guin, C., Fluid dynamics and detailed kinetic modeling of pollutant emissions from lean combustion systems (2010) Proceedings of the ASME Turbo Expo, pp. 451-459.

[13] Frassoldati, A., Cuoci, A., Faravelli, T., Ranzi, E., Colantuoni, S., Martino, P. D., et al. (2009). Experimental and modeling study of a low NOxcombustor for aero-engine turbofan. Combustion Science and Technology, 181(3), 483–495.

[14] Ng, C.N., CFD simulation of a gas turbine combustor, 2003, Carleton Institute for Mechanical and Aerospace Engineering: Ottawa (Canada).

[15] P.C. Hendrick, User experience with the Allison 250-C20R/1 turboshaft on the Belgian Army Agusta A109, presented at RTO AVT Symposium, Ottawa, Canada, 18-21 October 1999, published in NATO-RTO MP-34.

[16] E. Corporan, M. J. DeWitt, V. Belovich, R. Pawlik, A. C. Lynch, J. R. Gord, T. R. Meyer, Emissions Characteristics of a Turbine Engine and Research Combustor Burning a Fischer-Tropsch Jet Fuel, Energy & Fuels 2007, 21, 2615-2626.

[17] E. Corporan, M. DeWitt, M. Wagner, Evaluation of soot particulate mitigation additives in a T63 engine, Fuel Processing Technology 85 (2004) 727– 742.

[18] N. Bester, A. Yates, Assessment of the operational performance of Fischer–Tropsch synthetic–paraffinic kerosene in a T63 gas turbine compared to conventional jet a-1 fuel, Proceedings of ASME Turbo Expo 2009: Power for Land, Sea and Air, GT2009-60333, June 8-12, 2009, Orlando, Fl, USA.

[19] M. J. A. Islin, M. Cerza, P. E. Jenkins, An experimental study on the effects of Fischer-Tropsch (FT) blends with diesel #2 and JP5 on the performance of a Rolls-Royce model 250-C20B gas turbine engine, Proceedings of ASME Turbo Expo 2010: Power for Land, Sea and Air GT2010, paper 22436.

[20] D. Golden, M. Cerza, D. Myre, An Experimental Study of Water Injection into a Rolls-Royce Model 250-C20B Turboshaft Gas Turbine, paper AIAA 2008-4902, 44th AIAA/ASME/SAE/ASEE Joint Propulsion Conference & Exhibit 21 - 23 July 2008, Hartford, CT.

[21] W. Erhard, R. Gabler, A. Preiss, H. Rick, Monitoring and Control of Helicopter Engines at Abnormal Operating Conditions, Paper presented at the RTO AVT Symposium on "Design Principles and Methods for Aircrafl Gas Turbine Engines", held in Toulouse, France, 11-1.5 May 1998, published in RTO MP-8.

[22] Rolls-Royce Model 250-C20B/T63-A-720 and 250-C20R turboshaft engine Fact Sheets.

[23] Westbrook C.K., Dryer F.C., Prog. Energy Combust. Sci., 10:1 (1984).

[24] Honnet, S., et al., A surrogate fuel for kerosene. Proceedings of the Combustion Institute, 2009. 32: p. 485-492.

[25] T. Rindlisbacher, Guidance on the Determination of Helicopter Emissions, Federal Department of the Environment, Transport, Energy and Communications DETEC, Federal Office of Civil Aviation FOCA Division Aviation Policy and Strategy (2009), http://www.bazl.admin.ch/experten/regulation/03312/03419/03532/index.html.